PERGAMON

Nonlinear Analysis 41 (2000) 1029–1055

Nonlinear Analysis

www.elsevier.nl/locate/na

Phase-space structure and regularization of Manev-type problems

Florin Diacu [a,*], Vasile Mioc [b], Cristina Stoica [c]

[a] *Department of Mathematics and Statistics, University of Victoria, Victoria, Canada V8W 3P4*
[b] *Astronomical Institute of the Romanian Academy, Astronomical Observatory Cluj-Napoca, Str. Cireşilor 19, 3400 Cluj-Napoca, Romania*
[c] *Institute for Gravitation and Space Sciences, Laboratory for Gravitation, Str. Mendeleev 21-25, Bucharest, Romania*

Received 13 March 1998; accepted 9 September 1998

Keywords: Manev-type problems; Nonlinear particle dynamics; Relativity; Phase-space structure

0. Introduction

This paper brings a unifying point of view for several problems of nonlinear particle dynamics (including the classical Kepler, Coulomb, and Manev problems) by using the qualitative theory of dynamical systems. We consider two-body problems with potentials of the type $A/r + B/r^2$, where r is the distance between particles, and A, B are real constants. Using McGehee-type transformations and exploiting the rotational symmetry specific to this class of vector fields, we set the equations of motion in a reduced phase space and study all possible choices of the constants A and B. In this new setting the dynamics appears elegant and simple. In the end we use the phase-space structure to tackle the question of block-regularizing collisions, which asks whether orbits can be extended beyond the collision singularity in a physically meaningful way, i.e. by preserving the continuity of the general solution with respect to initial data.

0.1. History

The above class of problems is over three centuries old. Newton was the first to consider central-force and two-body problems in his monumental work *Principia*, whose

* Corresponding author. Tel.: 001-250-721-6330; fax: 001-250-721-8962.
E-mail address: diacu@math.uvic.ca (F. Diacu)

PII: S0362-546X(98)00326-5

first edition was published in 1687. But, in spite of their fame, these questions have taken a long time to be understood. Even the case $A>0$, $B=0$ of the Kepler problem has been solved as late as 1710 by Johann Bernoulli, not by Newton as it is traditionally believed, who had tackled only the elliptic case. Newton included the proof that the Kepler problem leads to conics in the second edition of *Principia*, published in 1713 (see [10]). It is less known, however, that Newton also considered the case $A, B>0$. In *Principia*'s Book I, Article IX, Proposition XLIV, Theorem XIV, Corollary 2, he showed that a central-force problem given by a potential of the type $A/r + B/r^2$, leads to a *precessionally elliptic* relative orbit. (This means that the trajectory of one particle – considered with respect to a fixed frame that has the other particle at its origin – is that of a point moving along an ellipse whose focal axis rotates in the plane of motion.) Newton's interest in this model was aroused by his failure to explain the Moon's orbit around the Earth within the framework of the classical inverse-square-force model. Except for the above property, Newton published no other results concerning this gravitational law. However, in the 1888-catalogue of the Portsmouth Collection of unpublished manuscripts, one can trace Newton's keen effort to understand the subject. After Newton, the potential $A/r+B/r^2$ was tackled by Alexis Clairaut, who finally abandoned it in favor of the classical one. In the second decade of our century, this model was used as a possible approximation of the field equations of general relativity (in a sense that will be made clear in Section 1) and succeeded to explain the observed perihelion advance of planet Mercury, which cannot be justified within the framework of the classical model. A few years later, the Bulgarian physicist Manev [18–21], proposed a similar gravitational model by taking $A=\mu$ and $B=3\mu^2/(2c^2)$ (μ and c being the gravitational parameter of the two-body system and the speed of light, respectively), bringing physical arguments in favor of this choice of the constants. Manev's arguments were based on the following facts.

In *Électricité et Optique*, published in 1901, Poincaré had noticed that Lorentz's theory concerning the electrodynamics of moving bodies, on which special relativity would be founded, failed to satisfy the action–reaction principle. Two years later, M. Abraham defined the *quantity of electromagnetic movement*, which helped Hasenöhrl prove the accuracy of Lorentz's contraction principle. In 1908, using this new quantity of electromagnetic movement, Max Planck stated a more general action–reaction principle, verified by special relativity, and from which Newton's third law followed as a theorem. Making use of those results, Manev showed that by applying the more general action–reaction principle to classical mechanics, he was naturally led to a law given by a potential of the type $A/r + B/r^2$. Thus, Manev considered this model as a substitute to general relativity. (We will point out in Section 1 that in a planetary approximation Manev's model is the natural classical analog of the Schwarzschild problem.) Therefore, Manev's theory seems rather suited to the needs of celestial mechanics than to those of cosmology, in which relativity has brought tremendous contribution. The advantage of Manev's model is that it explains solar-system phenomena with the same accuracy as relativity, but without leaving the framework of classical mechanics. Besides, 80 years of research have shown that relativity is powerless in defining a meaningful n-body problem. Though works like [14] and [17] have had important consequences in physics and even a notable impact in celestial mechanics (see [2]), they had never been

developed toward understanding the dynamics of gravitating particle systems, which has established itself as the fundamental problem in celestial mechanics, if not as "the most celebrated of all dynamical problems", as Whittaker put it in his treatise on the analytical dynamics of particles and rigid bodies [35, p. 339].

0.2. Recent developments

Unfortunately, Newton's treatment of the case $A, B > 0$ was far from complete. The false impression that Newton had exhausted the problem, and that this model had nothing but historical value, persisted (especially among physicists) until very recently (see, for example, Moulton's [27, Problem 4, p. 96] or Goldstein's [15, Problem 14, p. 123]). Using McGehee transformations, Delgado, Diacu, Lacomba, Mingarelli, Mioc, Perez, and Stoica understood the dynamics of the case $A, B > 0$ in 1996 (see [6]). Their paper appeared as a natural consequence of the recent interest in Manev's potential. Papers like [3,5,16,24,25] applied modern mathematical results (like KAM theory, the Melnikov method, etc.) as well as classical techniques, or went into the physical and astronomical significance of the model; for details regarding the specific results of these works see [6]. From the mathematical point of view, Manev's potential opens a new field of research; it has offered up to now surprising results concerning the dynamics of gravitational particles, which disagree with the classical ones when the motion takes place in the neighborhood of singularities (see [5, 6, 8, 9]). Thus Manev's law seems to build a bridge between classical mechanics and general relativity. The study of the n-body problem ($n \geq 3$) given by this potential appears to be a big challenge (see [9]).

0.3. Goal and methods

In the following sections we are mostly interested in the mathematical aspects of this class of potentials. We describe the global flow of the generalized Manev problem (i.e. the two-body problem given by the Manev potential for all possible choices of the real constants A and B) and then see, in case collisions occur, whether they are *block-regularizable*, i.e. whether the property of continuity of solutions with respect to initial data is preserved after collision. The first part uses McGehee transformations and the qualitative theory of dynamical systems, offering a way of unifying the Manev and Newton potentials (i.e. the cases $A, B > 0$ and $A > 0$, $B = 0$, respectively, which are – along with $A < 0$, $B \geq 0$ – the most important ones from the point of view of applications) by using a reduced phase-space description. This is possible due to the rotational symmetry Manev-type potentials have, which allows us to give a simple representation of these problems. The final part is based on the ideas advanced by Conley, Easton, and McGehee concerning the technique of surgery of isolated blocks and block-regularization of singularities (see [4, 12, 13, 22, 23]). It is important to note, however, that while the impossibility of regularizing collisions in particle-system dynamics has up to now been usually related to the nonexistence of an extension of a certain diffeoomorphism, this impossibility appears here generically because that extension is not unique.

0.4. Summary of results

In Section 1 we show that the natural classical analog of the Schwarzschild problem in the framework of the solar system is the Manev problem. This favors a strong connection between general relativity and Manev-type potentials. In Section 2 we obtain the analytic solution of the generalized Manev problem in closed form. Unfortunately, as it is the case for many nonlinear integrable systems, this formula offers no insight into the problem, so we continue with a qualitative analysis. In Section 3 we use McGehee-type transformations [22] to blow up the collision singularity (for the values of A and B for which singularities occur), and paste instead a so-called *collision manifold* to the phase space. The McGehee transformations are the key step in simplifying the problem. Due to the continuity of solutions with respect to initial data, the study of the (fictitious) flow on the collision manifold provides information about the local flow near collision. In this case, the regularized equations of motion allow us to give a full qualitative description of the global flow. We will see that the collision manifold is homeomorphic to a torus (embedded in the four-dimensional *full phase space*), on which the flow is foliated by periodic orbits, except for the upper and lower circles, which consist of degenerate equilibria. Since the flow has a rotational symmetry, we factorize it by S^1; consequently the four-dimensional phase space is factorized to a three-dimensional *reduced phase space*. Regarding the energy-integral constant as a parameter, we further determine the structure of the reduced phase space. Considering the energy integral in McGehee coordinates, we see that every energy level in the reduced phase space is part of a quadric surface, which degenerates in certain cases. Each energy level is itself foliated by orbits of different angular momenta. In the reduced phase space, the collision manifold is a circle of equilibria only if $B>0$. For $B=0$ the collision manifold becomes a point in the reduced phase space. For $B<0$ the system is free of collisions (a fact that has already been noticed by Saari [29]), so the collision manifold is the empty set.

In Sections 4–6 we describe the global flow in the reduced phase space with respect to the parameters A, B, the energy-integral constant h, and the angular momentum constant C. The flow for $B>0$ is given in Section 4. For $A>0$ the energy levels in the reduced phase space are portions of ellipsoids ($h<0$), paraboloids ($h=0$), and hyperboloids of one or two sheets or cones ($h>0$), as we have already seen in [6]. The physical motions correspond to both radial and spiral ejection–collision, ejection–escape, capture–collision, capture–escape, periodic, or quasiperiodic orbits. For $A=0$, in the reduced phase space we have portions of ellipsoids ($h<0$), cylinders ($h=0$), and hyperboloids of one sheet ($h>0$), with physical interpretations similar to those given in the previous case. For $A<0$ the energy levels are caps of ellipsoids and paraboloids for $h<0$ and $h=0$, respectively, and portions of hyperboloids (of one or two sheets) or cones of two sheets for $h>0$. There appear saddles outside the collision manifold for $h \geq A^2/(2B)$. Except for the periodic and quasiperiodic solutions, all previous motions occur in this case too; in addition, we obtain spiral and radial ejection – unstable-equilibrium, unstable-equilibrium – collision, unstable-equilibrium – escape, capture – unstable-equilibrium trajectories, unstable circular orbits, and unstable

rest points. Moreover, we find ejection–collision and capture–escape orbits coexisting for the same angular momentum.

In Section 5 we describe the global flow for $B=0$. If $A>0$ we are in the case of the Kepler problem. For $A=0$ we recover the classical results concerning the field-free motion of a particle. For $A<0$ the motion is possible only if $h>0$, and the orbits in the reduced phase space are branches of hyperbola, which physically correspond to capture–escape orbits.

In Section 6 we describe the global flow for $B<0$. In case $A>0$ the motion exists only for $h\geq A^2/(2B)$. In the reduced phase space the negative energy levels are ellipsoids, and the physical orbits correspond to periodic orbits. (If $h=A^2/(2B)$ the ellipsoids degenerate to a point, which physically means that the particle is at rest.) For zero angular momentum the motion is a radial libration. The zero and positive energy levels (which in the reduced phase space are paraboloids and upper sheets of hyperboloids of two sheets, respectively) correspond physically to infinity–infinity trajectories. If $A<0$ or $A=0$, the motion is possible only for $h>0$. In the reduced phase space the positive energy levels are upper sheets of hyperboloids of two sheets, and the corresponding physical orbits are of capture–escape type.

In Section 7 we prove a general theorem concerning the block-regularization of collision orbits, from which will follow that, for Manev-type potentials, collision singularities are, generically, not block-regularizable. The Newtonian case is an exception.

1. The Schwarzschild and the Manev problem

Einstein's general relativity replaced the view of classical mechanics, which regarded gravitation as a force in a three-dimensional space, with the idea that gravitation can be described by the intrinsic geometrical properties of the four-dimensional space-time manifold. More precisely, a solution of Einstein's *field equations* is a *line element*, i.e. the mathematical expression of the metric of the four-dimensional time-space manifold. In the particular case of the relativistic center-force problem (the relativistic analog of the classical Kepler problem), the solution of the field equations was obtained by Karl Schwarzschild in 1916 [31]. Therefore this problem bears Schwarzschild's name.

In this section we show that there is a strong connection between the Schwarzschild and the Manev problem, in what we will call *a planetary approximation*. Starting from the solution of the Schwarzschild problem, we see that the corresponding differential equations of the classical case are given by a Manev-type potential, i.e. one of the form $A/r+B/r^2$. Our derivation of this fact follows a classical idea (see, e.g., [1] for an elementary presentation or [26] for a modern one). Let us start by making the above notion precise.

Definition 1.1. A central-force problem is said to have a *planetary approximation* if the motion of the particle is periodic of period τ and $v=2\pi r/\tau$, where v is the tangential velocity of the particle, and r is its distance to the center.

The Schwarzschild line element in coordinates (t,r,θ,ϕ), where t is the time and (r,θ,ϕ) are the spatial spherical coordinates of the physical space, is the metric given by

$$ds^2=(c^2-2GM/r)\,dt^2-[c^2r/(c^2r-2GM)]\,dr^2-r^2\,d\theta^2-r^2\sin^2\theta\,d\phi^2,$$

where G is the gravitational constant, c is the speed of the light, and M is the mass of the field-generating body. To determine the orbit of the moving particle in the Schwarzschild problem, orbit which is given by a geodesic in the four-dimensional space-time manifold that has the above metric, we need to solve the variational problem $\delta\int ds=0$, which is equivalent to solving

$$\delta\int\left[(c^2-2GM/r)\left(\frac{dt}{ds}\right)^2-\frac{c^2r}{c^2r-2GM}\left(\frac{dr}{ds}\right)^2\right.$$
$$\left.-r^2\left(\frac{d\theta}{ds}\right)^2-r^2\sin^2\theta\left(\frac{d\phi}{ds}\right)^2\right]ds=0.$$

This means we must find the curve with fixed end points that extremises the above integral. We will now prove the following result:

Theorem 1.2. *In the solar-system approximation, the equations of motion describing the motion of a particle in the relativistic Schwarzschild problem have the same form as the Binet-type system of the central-force problem given by the Manev-type potential.*

Remark. *By a Manev-type potential we understand a function of the type $A/r+B/r^2$. The notion of Binet-type equation will be made clear during the proof.*

Proof. A standard result of the calculus of variations states that the above variational problem is equivalent to finding the solution of the corresponding Euler–Lagrange equations, which in our case take the form

$$\begin{aligned}
&\frac{d}{ds}\left(r^2\frac{d\theta}{ds}\right)=r^2\sin\theta\cos\theta\left(\frac{d\phi}{ds}\right)^2,\\
&\frac{d}{ds}\left(r^2\sin^2\theta\frac{d\phi}{ds}\right)=0,\\
&\frac{d}{ds}\left[(c^2-2GM/r)\frac{dt}{ds}\right]=0,\\
&(c^2-2GM/r)\left(\frac{dt}{ds}\right)^2-\frac{c^2r}{c^2r-2GM}\left(\frac{dr}{ds}\right)^2-r^2\left(\frac{d\theta}{ds}\right)^2-r^2\sin^2\theta\left(\frac{d\phi}{ds}\right)^2=1,
\end{aligned}\tag{1.1}$$

where the unknowns t, r, θ, ϕ, dt/ds, dr/ds, $d\theta/ds$, $d\phi/ds$ are functions of s. Our immediate goal is to reduce this system to a differential equation involving the variables r and dr/ds alone. This will be done by finding two first integrals.

For suitable initial conditions, standard results of differential equations theory assure the existence and uniqueness of a solution $\gamma=(t,r,\theta,\phi,\mathrm{d}t/\mathrm{d}s,\mathrm{d}r/\mathrm{d}s,\mathrm{d}\theta/\mathrm{d}s,\mathrm{d}\phi/\mathrm{d}s)$ of Eqs. (1.1). Let us now see that the set $\Gamma=\{\gamma\mid\theta=\pi/2,\mathrm{d}\theta/\mathrm{d}s=0\}$ is invariant for Eqs. (1.1). This means that if $\gamma(s_0)$ belongs to Γ, where s_0 is an initial value for the independent variable s, then $\gamma(s)$ belongs to Γ for all values s for which γ is defined. Indeed, the invariance of Γ follows from the first equation in Eqs. (1.1): for $\theta(s_0)=\pi/2$ and $(\mathrm{d}\theta/\mathrm{d}s)(s_0)=0$, we have $\theta(s)=\pi/2$ and $(\mathrm{d}\theta/\mathrm{d}s)(s)=0$.

Let us now restrict Eqs. (1.1) to the invariant set Γ. Then the second equation in Eqs. (1.1) is easy to integrate; we obtain the relation

$$r^2(\mathrm{d}\phi/\mathrm{d}s)=\alpha\ (\text{constant}),\tag{1.2}$$

which is a first integral for Eqs. (1.1). The third equation in Eqs. (1.1) is also easy to integrate; we obtain the relation

$$[1-2GM/(c^2r)](\mathrm{d}t/\mathrm{d}s)=\beta\ (\text{constant}),\tag{1.3}$$

which is also a first integral for Eqs. (1.1). Using Eqs. (1.2) and (1.3), the last equation in Eqs. (1.1) restricted to Γ takes the form

$$\frac{\beta^2c^4r}{c^2r-2GM}-\frac{c^2r}{c^2r-2GM}\left(\frac{\mathrm{d}r}{\mathrm{d}s}\right)^2-\left(\frac{\alpha}{r}\right)^2=1,\tag{1.4}$$

which is a relation between r and $\mathrm{d}r/\mathrm{d}s$ alone. Let us simplify now Eq. (1.4). For this we make ϕ play the role of the independent variable. Abusing the notation, we denote by r the function that depends on the ϕ-variable. Prime will denote differentiation with respect to ϕ, so $r'=\mathrm{d}r/\mathrm{d}\phi$. From Eq. (1.2) we then obtain $\mathrm{d}r/\mathrm{d}s=(\alpha/r^2)r'$, and Eq. (1.4) becomes

$$\frac{\alpha^2}{r^4}(r')^2+\frac{\alpha^2}{r^2}-\frac{2GM\alpha^2}{c^2r^3}-\frac{2GM}{c^2r}=\beta^2c^2-1.\tag{1.5}$$

The change of variable $r=1/u$ transforms Eq. (1.5) into

$$(u')^2=\frac{2GM}{c^2}u^3-u^2+\frac{2GM}{\alpha^2c^2}u+\frac{\beta^2c^2-1}{\alpha^2},\tag{1.6}$$

which, if differentiated with respect to ϕ, yields

$$u'\left(u''-\frac{3GM}{c^2}u^2+u-\frac{GM}{\alpha^2c^2}\right)=0.\tag{1.7}$$

Two equations arise from here. The first one, $u'=0$, leads to $r=\text{constant}$, i.e. circular periodic solutions like in the classical case. The second equation,

$$u''=\frac{3GM}{c^2}u^2-u+\frac{GM}{\alpha^2c^2},\tag{1.8}$$

is similar to the Binet equation that describes the motion of a particle in a central-force field (the part of the constant angular momentum being played by the quantity αc; see Eq. (1.2)). More precisely, it would correspond to the Binet equation having

the potential $U(r) = GM/r + \alpha^2 GM/r^3$. If we denote by v the tangential velocity of the particle and use the fact that α^2/r^2 is equal to v^2/c^2, the potential can be approximated by $U(r) = (GM/r)[1 + (v/c)^2]$. Most orbits in the solar system are almost circular (planets, satellites, most asteroids, many comets), so we can assume that $v = 2\pi r/\tau$, where τ is the period of revolution of the particle. We are thus in the hypotheses of the planetary approximation given in Definition 1.1. Also, by Kepler's third law, $r(v/c)^2 = \mu$, where μ is the same constant for all mentioned bodies. Thus, the potential can be approximated by $U(r) = GM/r + \mu GM/r^2$, which is of the form $A/r + B/r^2$, i.e. of Manev type. This completes the proof.

Remark. *We do not claim that the above theorem proves that the Schwarzschild solution leads to the Manev-type potential via the planetary approximation. The statement that Eq.* (1.8) *were given by the potential* $U(r) = GM/r + \alpha^2 GM/r^3$ *would be wrong. The reason is that Eq.* (1.8) *was obtained in the framework of relativity, whereas the concept of the Binet-type equation belongs to classical mechanics. Such a statement would mean applying results of one model, with some kind of hypotheses, to another model, in which other hypotheses reign. Therefore, the conclusion of Theorem* 1.2 *is that, within the framework of classical mechanics and in a planetary approximation, the* natural analog *of the relativistic gravitational theory is the law of Manev. Besides Manev's physical arguments in favor of this gravitational model, the above theorem shows the importance of understanding the mathematics of the Manev-type potential.*

In the following sections we will apply the qualitative methods of dynamical systems theory to investigate the dynamics of Manev-type potentials $A/r + B/r^2$ for all possible real values of the constants A and B.

2. The general solution

The equations of motion of the Manev-type problem are given by the Hamiltonian system

$$\dot{\mathbf{q}} = \partial H(\mathbf{q}, \mathbf{p})/\partial \mathbf{p}, \qquad \dot{\mathbf{p}} = -\partial H(\mathbf{q}, \mathbf{p})/\partial \mathbf{q}, \tag{2.1}$$

where $\mathbf{q} = (\mathbf{q}_1, \mathbf{q}_2)$ is the configuration of the system, $\mathbf{q}_1, \mathbf{q}_2$ are the position vectors of the two particles with respect to an absolute frame, $\mathbf{p} = (\mathbf{p}_1, \mathbf{p}_2)$ is the momentum of the system, $\mathbf{p}_1, \mathbf{p}_2$ are the momenta of the two particles, the dot represents differentiation with respect to the time variable, and H is the Hamiltonian function

$$H(\mathbf{q}, \mathbf{p}) = (\mathbf{p}_1^{\mathrm{T}}\mathbf{p}_1 + \mathbf{p}_2^{\mathrm{T}}\mathbf{p}_2)/2 - A/|\mathbf{q}_2 - \mathbf{q}_1| - B/|\mathbf{q}_2 - \mathbf{q}_1|^2, \tag{2.2}$$

(T denoting transposition), which yields the integral of energy

$$H(\mathbf{q}, \mathbf{p}) = h/2, \tag{2.3}$$

where h is the energy constant.

Since H depends only on the relative positions $\mathbf{q}_2 - \mathbf{q}_1$ and not on the position vectors $\mathbf{q}_1$ and $\mathbf{q}_2$, the Manev-type problem can be reduced to a central-force problem by introducing the relative coordinates $\mathbf{r} = \mathbf{q}_2 - \mathbf{q}_1$. Eqs. (2.1) take the form

$$\dot{\mathbf{r}} = \partial H(\mathbf{r}, \mathbf{p})/\partial \mathbf{p}, \qquad \dot{\mathbf{p}} = -\partial H(\mathbf{r}, \mathbf{p})/\partial \mathbf{r}, \tag{2.4}$$

where

$$H(\mathbf{r}, \mathbf{p}) = (\mathbf{p}^{\mathrm{T}}\mathbf{p})/2 - A/|\mathbf{r}| - B/|\mathbf{r}|^2. \tag{2.5}$$

Eliminating the momentum, Eq. (2.3) form the second-order system

$$\ddot{\mathbf{r}} = -(A/r^3 + 2B/r^4)\mathbf{r}, \tag{2.6}$$

where $r = |\mathbf{r}|$. In polar coordinates (r, u), Eqs. (2.6) become

$$\begin{aligned} &\ddot{r} - r\dot{u}^2 = -A/r^2 - 2B/r^3, \\ &r\ddot{u} + 2\dot{r}\dot{u} = 0. \end{aligned} \tag{2.7}$$

The second equation of Eq. (2.7) yields the angular-momentum integral

$$r^2\dot{u} = C, \tag{2.8}$$

where C is the constant of the angular momentum. In the new polar coordinates, the integral of energy (2.3) takes the form

$$\dot{r}^2 + r^2\dot{u}^2 - 2A/r - 2B/r^2 = h. \tag{2.9}$$

To obtain the solution of system (2.7), let us first take some initial data $(r, u, \dot{r}, \dot{u})(t_0) = (r_0, u_0, \dot{r}_0, \dot{u}_0)$. Using the integrals of the system (see [6]) in the nonrectilinear case $C \neq 0$, Eqs. (2.7) can be reduced to the Binet-type equation

$$d^2(1/r)/\mathrm{d}u^2 + (1 - 2B/C^2)(1/r) = A/C^2. \tag{2.10}$$

Depending on the sign of the parameter $(1 - 2B/C^2)$, the solution of Eq. (2.10), for initial conditions $(1/r, \mathrm{d}(1/r)/\mathrm{d}u)(u_0) = (1/r_0, -\dot{r}_0/C)$, takes the form

$$r(u) = [(r_0^{-1} + A(2B - C^2)^{-1})\tilde{C}(u) - \dot{r}_0(2B - C^2)^{-1/2}\tilde{S}(u) - A/(2B - C^2)]^{-1}, \tag{2.11}$$

$$r(u) = [(A/2)C^{-2}(u - u_0)^2 - \dot{r}_0C^{-1}(u - u_0) + r_0^{-1}]^{-1}, \tag{2.12}$$

$$r(u) = [(r_0^{-1} + A(2B - C^2)^{-1})\bar{C}(u) - \dot{r}_0(C^2 - 2B)^{-1/2}\bar{S}(u) - A/(2B - C^2)]^{-1}, \tag{2.13}$$

for $C^2 < 2B$, $C^2 = 2B$, and $C^2 > 2B$, respectively, where $(\tilde{S}, \tilde{C}) = (\sinh, \cosh)((2BC^{-2} - 1)^{1/2}(u - u_0))$ and $(\bar{S}, \bar{C}) = (\sin, \cos)((1 - 2BC^{-2})^{1/2}(u - u_0))$.

Eqs. (2.11)–(2.13), which can also be obtained using a classical perturbative approach (see [6]), offer the general solution of the nonrectilinear Manev-type problem

in closed form, assuming that r_0 and $\dot{r}_0$ take all admissible real values. Unfortunately, this precise but tangled formula is of little help in understanding the motion for different values of the initial conditions. Therefore, we will now proceed with a qualitative approach, which will put into the evidence the dynamical elegance and simplicity of the class of differential equations we study here.

3. Blow-up and reduction

Let us now start our qualitative endeavors of the equations of motion (2.7). The collision singularity, which occurs if and only if $r = 0$, will be blown up by using McGehee-type transformations (for more details see [6, 11]). By formally multiplying the energy integral (2.9) by r^2 (a rigorous justification of this step is given in [11]), we obtain the relation

$$(r\dot{r})^2 + (r^2\dot{u})^2 = hr^2 + 2Ar + 2B. \tag{3.1}$$

Then we consider the transformations $x = r\dot{r}$, $y = r^2\dot{u}$, rescale the time through the independent-variable transformation $\mathrm{d}t = r^2\,\mathrm{d}s$, and obtain, after a straightforward computation, the new equations of motion:

$$r' = rx, \qquad x' = r(hr + A), \qquad u' = y, \qquad y' = 0, \tag{3.2}$$

where the prime denotes differentiation with respect to the new (fictitious) time variable s. The energy relation (3.1) and the angular-momentum integral are now given by the equations:

$$x^2 + y^2 = hr^2 + 2Ar + 2B, \tag{3.3}$$

$$y = C = \text{constant}. \tag{3.4}$$

Notice that Eqs. (3.2) and the relations (3.3)–(3.4) are well defined if $r = 0$. This means that we can extend the phase space to contain the invariant manifold $\{(r, x, u, y) \,|\, r = 0\}$. Though having no real physical significance, the flow on this invariant manifold will let us understand the behavior of the flow near collision. This is possible due to the continuity of the flow with respect to initial data.

Let us now define the *collision manifold* CM by intersecting the sets $\{(r, x, u, y) \,|\, r = 0\}$ and $\{(r, x, u, y) \,|\, x^2 + y^2 = hr^2 + 2Ar + 2B\}$; we thus obtain the subspace

$$CM = \{(r, x, u, y) \,|\, x^2 + y^2 = 2B\},$$

which, if $B > 0$, is a 2-torus in the three-dimensional space of the coordinates $(x, u, y) \in \mathbb{R} \times [0, 2\pi] \times \mathbb{R}$, because it forms a cylinder whose caps, at $u = 0$ and $u = 2\pi$, are identified.

The flow on CM is simple: it consists of periodic orbits if $y \neq 0$, and of circles formed by degenerate equilibria if $y = 0$, case in which $x = \pm\sqrt{2B}$. We can, in fact, determine the flow near the collision manifold, as it was done in [11] for $A, B > 0$. However, that approach is restricted to a local description. In order to find the global flow, we will use the following observation.

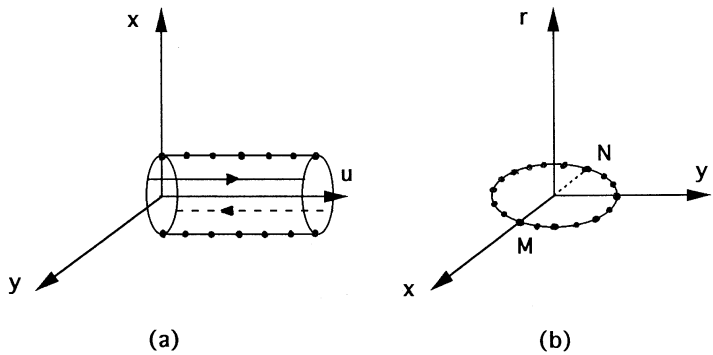

Fig. 1. The collision-manifold as (a) a torus in (x, y, u)-coordinates and as (b) a circle in the reduced phase space, both for $B>0$.

Since the variable u does not appear explicitly in the vector field (3.2) and in the relations (3.3) and (3.4), it means that the flow is invariant to rotations, so we can factorize it by S^1. In this case the collision manifold CM becomes a circle in the three-dimensional space of the coordinates $(r; x, y) \in \mathbb{R}_+ \times \mathbb{R}^2$, where $\mathbb{R}_+ = \{r \geq 0\}$ (see Fig. 1), which we will from now on call *reduced phase space*. The points M and N on this circle represent the circles of equilibria on the torus; the other points on the collision-manifold circle correspond to the periodic orbits on the torus.

If $B=0$, CM is a point in the reduced phase space, and if $B<0$ the collision manifold is the empty set (i.e. collisions do not occur). This last result has already been established by Saari [29] in a different context and with a different method.

In the following sections we will describe the flow of Eqs. (3.2)–(3.4) in the reduced phase space and give the physical interpretation of the solutions.

Note. We will abuse the terminology by further calling *equilibria*, *periodic orbits*, etc., what appear to be such orbits in the reduced phase space. Of course, in full phase space these must be regarded $\times S^1$, i.e. as manifolds of solutions. For example, an equilibrium in the reduced phase space is a periodic orbit or a circle formed by full-phase-space equilibria; a periodic orbit in the reduced phase space is an invariant torus of solutions, etc.

4. The flow for $B>0$

4.1. The case $A>0$

The dynamics of this case was considered in [6]. We will revisit it here.

4.1.1. Negative energy

Eq. (3.3) shows that in the reduced phase space, every negative energy level ($h<0$) is an ellipsoid with the lower cap removed, since $r \geq 0$ implies that the collision circle intersects this ellipsoid below the "equator" (see Fig. 2).

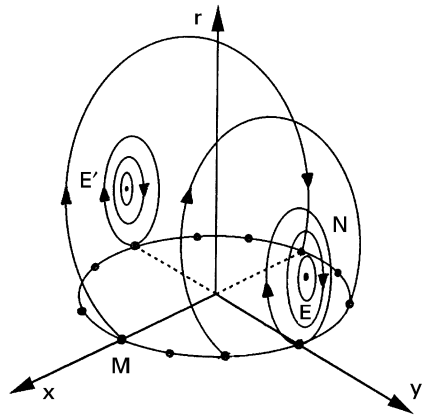

Fig. 2. The flow in reduced phase space for $B>0$, $A>0$, $h<0$.

There are two equilibria, E and E', outside the collision circle, whose coordinates are given by $r=-A/h$, $x=0$, $y=\pm\sqrt{2B-A^2/h}$. For $\sqrt{2B}<|y|<\sqrt{2B-A^2/h}$, the orbits are periodic, for $|y|=\sqrt{2B}$, they are homoclinic, while for $|y|<\sqrt{2B}$ they are heteroclinic. The heteroclinic orbit connecting M and N (see Fig. 2) corresponds physically to orbits ejecting radially and then ending radially in a collision. The other heteroclinic orbits in Fig. 2 (as well as the two homoclinic orbits) correspond to spiraling ejection-collision trajectories.

The cycles of Fig. 2 correspond to orbits on tori $S^1\times S^1$ in full phase space. The flow on each torus is linear. An orbit of this kind is either periodic (when the frequency ratio is rational) or quasiperiodic (in case the frequency ratio is irrational). The frequency ratio T/y, where T represents the period, can be obtained using the same method as in [6], and is given by the formula

$$\frac{T}{y}=\frac{2\pi-4\arctan\sqrt{A^2/h(2B-y^2)-1}}{y\sqrt{y^2-2B}}. \tag{4.1}$$

This means that, for a fixed y, except for a set of values of measure zero, all orbits are quasiperiodic. This allows one to apply the classical results of KAM theory, as it has been done in [16].

Finally, the two equilibria in the reduced phase space lying outside the collision-manifold circle correspond physically to stable circular orbits.

4.1.2. Zero energy

In this case the energy relation (3.3) becomes

$$x^2+y^2-2Ar=2B, \tag{4.2}$$

which shows that in the reduced phase space the zero energy level is a paraboloid with the cap removed (see Fig. 3). Notice that the cap is removed because of the condition

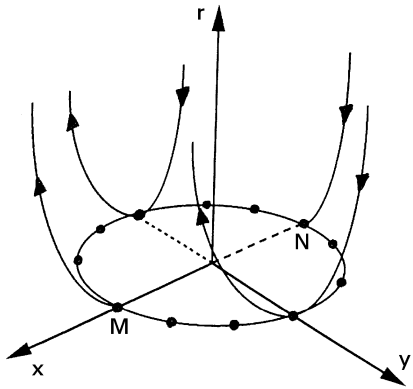

Fig. 3. The flow in the reduced phase space for $B>0$, $A>0$ and $h=0$.

$r \geq 0$. There are no equilibria outside the collision-manifold circle and the orbits are parabolas if $|y| \geq \sqrt{2B}$ or arcs of parabolas if $|y| < \sqrt{2B}$.

Each parabola of the case $|y| > \sqrt{2B}$ corresponds physically to collision free precessional parabolic orbits with asymptotic velocity zero at infinity, whereas each curve of the case $|y| \leq \sqrt{2B}$, $y \neq 0$, corresponds to either collision or ejection precessional parabolic orbits with asymptotic velocity zero at infinity. The arcs of parabola for which $y=0$ represent radial ejection or collision orbits with asymptotic velocity zero at infinity.

4.1.3. Positive energy

In this case it is more convenient to write the energy relation (3.3) as

$$x^2 + y^2 - h(r + A/h)^2 = 2B - A^2/h, \tag{4.3}$$

a formula which shows that we have three distinct situations to analyze, depending on the sign of the quantity $h - A^2/(2B)$.

If $h < A^2/(2B)$, from Eq. (4.3) we see that every energy level in the reduced phase space is a hyperboloid of two sheets intersected with the half-space $r \geq 0$; this last condition removes the lower sheet and the cap of the upper sheet (see Fig. 4a). Since $y = C$, this surface is foliated by branches of hyperbola for $y \geq \sqrt{2B}$ or $y \leq -\sqrt{2B}$, and by arcs of branches of hyperbola for $|y| < \sqrt{2B}$. The physical interpretation of the orbits represented in this case is similar to the one described in Section 4.1.2, with the differences that precessional parabolas are replaced with precessional hyperbolas and that the asymptotic velocity at infinity is now positive, namely $\sqrt{h}$.

In case $h = A^2/(2B)$, every energy level in the reduced phase space is a cone of two sheets intersected with the half-space $r \geq 0$; this intersection removes the lower sheet and the cap of the upper sheet (see Fig. 4b). The orbits are the same as in the previous case $h < A^2/(2B)$, except for those going through M and N, which are half-lines. The physical interpretation is the same as for $h < A^2/(2B)$.

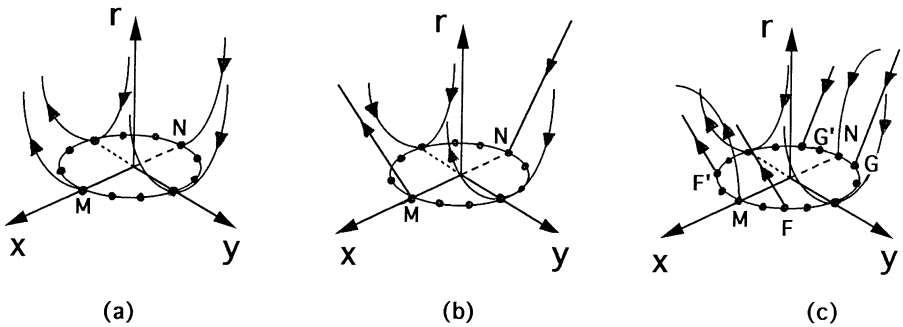

Fig. 4. The flow in the reduced phase space for $B>0$, $A>0$ and (a) $h<A^2/(2B)$, (b) $h=A^2/(2B)$, and (c) $h>A^2/(2B)$, respectively.

In case $h>A^2/(2B)$, every energy level in the reduced phase space is a hyperboloid of one sheet intersected with the half space $r\geq 0$ above the "equator"; this intersection removes the lower part of the hyperboloid. The orbits are branches of hyperbola for $y\geq\sqrt{2B}$ or $y\leq-\sqrt{2B}$, arcs of branches of hyperbola for $\sqrt{2B-A^2/h}<|y|<2B$, two pairs of half-lines (ejecting from F,F' and tending to G,G') for $y=\sqrt{2B-A^2/h}$, and arcs of branches of hyperbolas (conjugate to those corresponding to $y>\sqrt{2B-A^2/h}$ or $y<-\sqrt{2B-A^2/h}$) for $|y|<\sqrt{2B-A^2/h}$. The physical interpretation is the same as for $h<A^2/(2B)$.

Also note that, as in the zero-energy case 4.1.2, if $h>0$ there are no equilibria outside the collision manifold.

4.2. The case $A=0$

This is the case of the inverse cubic attractive force, which was studied starting with Newton; in fact it seems to have been the first case for which the occurrence of collisions for nonzero angular momenta was noticed (see [36]). The energy relation (3.3) reduces here to

$$x^2+y^2-hr^2=2B. \tag{4.4}$$

Again, the topology of each energy level depends on the sign of the energy constant h.

4.2.1. Negative energy

Eq. (4.4) shows that in the reduced phase space every negative energy level is the upper half of an ellipsoid, since the collision-manifold circle coincides with the "equator" of the ellipsoid (see Fig. 5a). Consequently, there are no equilibria outside the collision-manifold circle. All orbits fulfill the condition $|y|<\sqrt{2B}$ and are heteroclinic. They correspond physically to spiral or radial ejection-collision orbits. The points $x=0$, $y=\pm\sqrt{2B}$ on the collision-manifold circle represent degenerate orbits which start at collision and remain at collision for all time. We shall meet again such degenerate solutions in the Sections 4.2.2, 4.3.1–4.3.3 below.

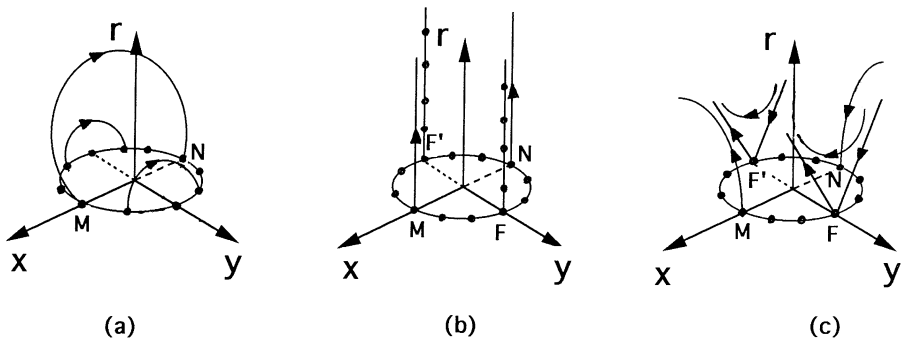

Fig. 5. The flow in the reduced phase space for $B>0$, $A=0$ and (a) $h<0$, (b) $h=0$, and (c) $h>0$, respectively.

4.2.2. Zero energy

The energy relation (4.4) is

$$x^2 + y^2 = 2B,$$

so the zero energy level in the reduced phase space is a cylinder intersected with the half-space $r \geq 0$. All orbits are generatrices of the cylinder (see Fig. 5b), except for those corresponding to $|y| = \sqrt{2B}$, which are lines consisting of equilibria (the lines through F and F' in Fig. 5b). These equilibria physically represent stable circular orbits around the center. (In particular, F and F' are degenerate solutions which remain in collision for all time.) The other generatrices of Fig. 5b physically represent spiral ejection-escape or infinity-collision orbits, except for the two generatrices through M and N, which represent radial orbits of the same type. In each case the asymptotic velocity at infinity is zero.

4.2.3. Positive energy

In this case, relation (4.4) shows that in the reduced phase space every positive energy level is a hyperboloid of one sheet intersected with the half-space $r \geq 0$ following its "equator" (see Fig. 5c). There are no equilibria outside the collision-manifold circle. The orbits are branches of hyperbolas for $y < -\sqrt{2B}$ or $y > \sqrt{2B}$, two pairs of lines (ejecting from and tending to F and F') for $|y| = \sqrt{2B}$, and arcs of branches of hyperbolas (conjugate with respect to those for which $y < -\sqrt{2B}$ or $y > \sqrt{2B}$) for $|y| < \sqrt{2B}$. The physical interpretation of these orbits is similar to the ones discussed in Section 4.1.3 for $h > A^2/(2B)$.

4.3. The case $A<0$

This case exhibits several interesting dynamical aspects, especially for positive energy levels.

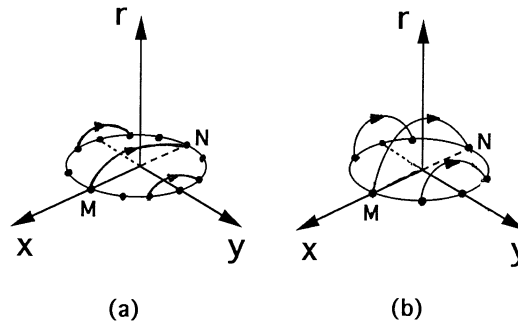

Fig. 6. The flow in the reduced phase space for $B>0$, $A<0$ and (a) $h<0$ and (b) $h=0$, respectively.

4.3.1. Negative energy

According to Eq. (4.3), every negative energy level in the reduced phase space is the upper cap of an ellipsoid: the collision-manifold circle intersects the surface above the "equator" (see Fig. 6a), hence there are no equilibria outside the collision-manifold circle. All the orbits are heteroclinic arcs of ellipse that connect equilibria of the collision-manifold circle. The physical interpretation is as the one described in Section 4.2.1.

4.3.2. Zero energy

The energy relation (3.3) reduces to Eq. (4.2) with $A<0$, which shows that in the reduced phase space the zero energy level is the cap of a paraboloid (see Fig. 6b). The integral $y=C$ foliates the surface in arcs of parabola, so all orbits are heteroclinic, and there are no equilibria outside the collision-manifold circle. The physical interpretation is the same as in Section 4.3.1.

4.3.3. Positive energy

These manifolds present dynamical aspects that did not occur in the previous cases. Our discussion will follow three subcases according to the sign of $h-A^2/(2B)$.

(a) If $h<A^2/(2B)$, Eq. (4.3) shows that every energy level in the reduced phase space is a hyperboloid of two sheets intersected with the half-space $r\geq 0$ (see Fig. 7a). There are no equilibria outside the collision-manifold circle. The orbits are upper branches of hyperbola if $y\leq -\sqrt{2B}$ or $y\geq \sqrt{2B}$, and upper branches of hyperbola or arcs of lower branches if $|y|<\sqrt{2B}$. All lower-branch arcs correspond to heteroclinic orbits between equilibria of the collision-manifold circle. Physically, these orbits are spiral or radial ejection–collision orbits. Each upper branch of hyperbola represents solutions that come from infinity and tend to infinity, without encountering collisions. The asymptotic velocity at infinity is positive.

Let us take a closer look at the physical motion in this case. Since $B>0$ and $A<0$, the acting force is the sum of a repulsive inverse-square force and an attracting inverse-cubic force. For small distances, the attractive force is dominant, whereas for large

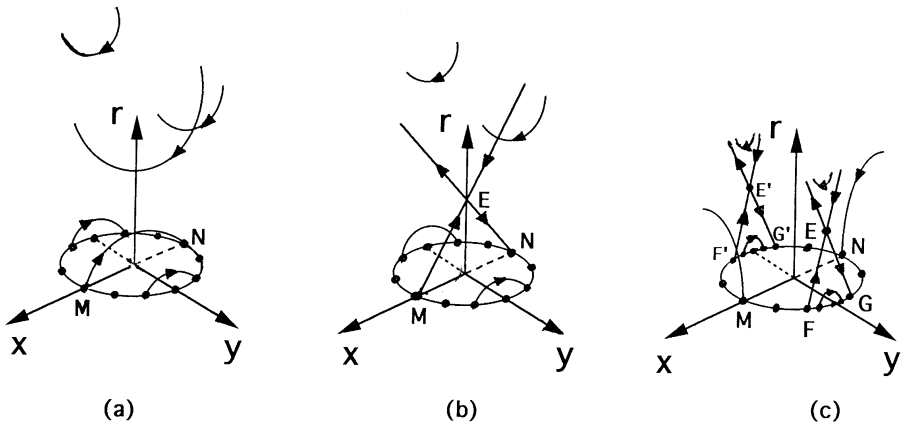

Fig. 7. The flow in the reduced phase space for $B>0$, $A<0$ and $h>0$, with (a) $h<A^2/(2B)$, (b) $h=A^2/(2B)$, and (c) $h>A^2/(2B)$, respectively.

distances, the repulsive one prevails. We have seen in Sections 4.3.1 and 4.3.2, that a particle with nonnegative energy is bounded and always ends in a collision. If the energy is positive, there occurs a new situation: for initial data far enough from the center, the dominant repulsive force gives rise to a capture–escape orbit. Fig. 7a shows that for $h<A^2/(2B)$ the physical plane of motion contains an annulus-shaped "forbidden zone", which – due to insufficient energy – the particle cannot cross. The radii of the small and big circle defining this annulus are $r_1=-(A+\sqrt{A^2-2Bh})/h$ and $r_2=-(A-\sqrt{A^2-2Bh})/h$, respectively. If the particle ejects from collision (spiralling or radially), it reaches the circle of radius r_1 from the inside, then returns and collides with the center. If the particle comes from infinity (spiralling or radially), it reaches the circle of radius r_2 from the outside, then tends back to infinity. Moreover, if the angular momentum is such that $y<-\sqrt{2B}$ or $y>\sqrt{2B}$, then collisions do not occur (as in the corresponding situations occurring in Sections 4.1.2, 4.1.3, and 4.2.3 above).

(b) If $h=A^2/(2B)$, Eq. (4.3) shows that in the reduced phase space the energy level is a cone of two sheets intersected with the half-space $r\geq 0$, i.e. the upper sheet of the cone and the cap of the lower sheet. This surface is foliated by $y=C$ as in case (a) discussed before: the same curves for the same values of y, with the same corresponding solutions in full phase space. There is, however, a new situation, which occurs for $y=0$: a pair of half-lines ending in M and N, which intersect each other in E (see Fig. 7b). E is an unstable equilibrium located outside the collision-manifold circle, namely at $r=-A/h=-2B/A$, $x=0$, $y=0$. In full phase space it corresponds to a circle in the plane $x=0$ formed by unstable equilibria. Physically, these equilibria are unstable rest points located at a distance $r=-2B/A$ from the center.

The heteroclinic orbits ME and EN correspond physically to radial orbits which either eject from a collision and tend to rest at distance $r=-2B/A$ from the center or are initially at that distance and tend to collision. The half-lines above E in Fig. 7b represent physically orbits that either come radially from infinity and tend to rest at a distance $r=-2B/A$ from the center, or move in the opposite direction.

(c) If $h>A^2/(2B)$, Eq. (4.3) shows that every energy level in the reduced phase space is a hyperboloid of one sheet intersected with the half-space $r\geq 0$ below the "equator" (see Fig. 7c). Again, the first integral $y=C$ foliates this surface in invariant sets. For $y\leq -\sqrt{2B}$ or $y\geq\sqrt{2B}$, the orbits are upper branches of hyperbola. For $\sqrt{2B-A^2/h}<|y|<\sqrt{2B}$, the orbits are upper branches of hyperbola or arcs of lower branches of hyperbola. For $|y|=\sqrt{2B-A^2/h}$, the orbits are two pairs of half-lines (one pair ending in F and G with reciprocal intersection in E, the other pair ending in F' and G' with reciprocal intersection in E'. The two equilibria E and E' that lie outside the collision-manifold circle have coordinates $r=-A/h$, $x=0$, $y=\pm\sqrt{2B-A^2/h}$. Both are saddles. For $|y|<\sqrt{2B-A^2/h}$, the orbits are arcs of branches of hyperbola conjugate to the above hyperbolas.

The two arcs of branches of hyperbola through M and N in Fig. 7c (for which $y=0$) as well as the other arcs of branches of hyperbola (for which $0<|y|<\sqrt{2B-A^2/h}$) have the same physical interpretation as the corresponding arcs in Fig. 5c. In each case the asymptotic velocity at infinity is positive. The equilibria E and E' correspond physically to unstable circular orbits at distance $r=-A/h$ from the center. The orbits $FE, F'E', EG$, and $E'G'$ correspond physically to spiraling orbits that eject from collision and tend to the unstable circular motion of radius $-A/h$, or conversely. The half-lines above E and E' correspond physically to orbits that spiral inward from infinity toward the unstable circular motion at distance $-A/h$ from the center, or conversely, with positive asymptotic velocity at infinity. The arcs of lower branches of hyperbola (for $\sqrt{2B-A^2/h}<|y|<\sqrt{2B}$) and upper branches of hyperbola (for $|y|>\sqrt{2B-A^2/h}$) have the same physical interpretation as those in case (b) above.

5. The flow for $B=0$

This case contains the well-known flow of the Newtonian and Coulomb equations as well as the trivial case of a force-free field; it is however worthwhile looking at them from the perspective of the reduced phase space within the framework of this unifying representation.

5.1. The case $A>0$

This is the Newtonian central-force problem. Eq. (3.3) takes the form

$$x^2+y^2-2Ar-hr^2=0, \tag{5.1}$$

and the corresponding reduced phase space pictures appear as in Fig. 8, in which the collision manifold is reduced to a point, the case $h<0$ gives rise to ellipses, the case $h=0$ to parabolas, and the case $h>0$ to hyperbolas. In full phase space the collision-manifold is a circle and all the well-known solutions of the Newtonian central-force problem are recovered.

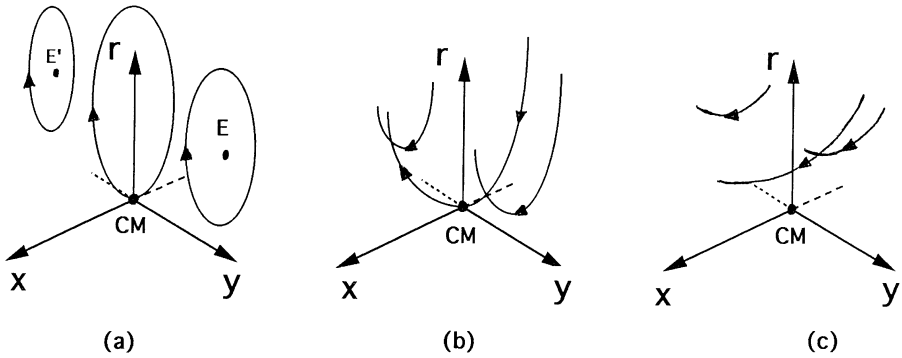

Fig. 8. The flow in the reduced phase space for the Newtonian case $B=0$, $A>0$, and (a) $h<0$, (b) $h=0$, and (c) $h>0$, respectively.

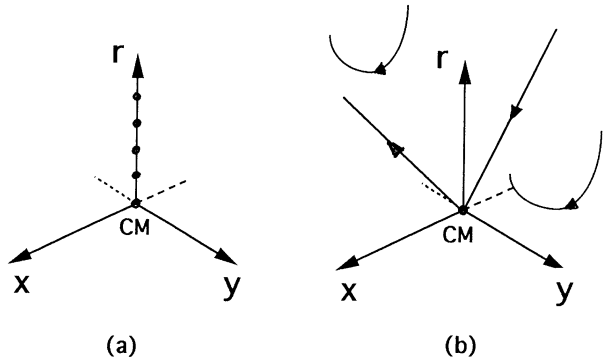

Fig. 9. The flow in the reduced phase space for $B=0$, $A=0$, and (a) $h=0$ and (b) $h>0$, respectively.

5.2. *The case* $A=0$

In this degenerate case the force field vanishes and the energy relation (3.3) takes the form

$$x^2+y^2-hr^2=0.$$

If $h<0$ this relation represents an imaginary cone, so real motion is impossible. If $h=0$, the reduced phase space is the half-line $r\geq 0$, $x=y=0$, formed by equilibria as Fig. 9a shows. Physically, the particle is at all time at rest with respect to the center. In particular an orbit starting at collision remains at collision for all time. If $h>0$, every energy level in the reduced phase space is the upper sheet of a cone with the vertex at the collision-manifold point (see Fig. 9b). Physically, the motion is rectilinear and uniform (radial for $y=0$, nonradial otherwise).

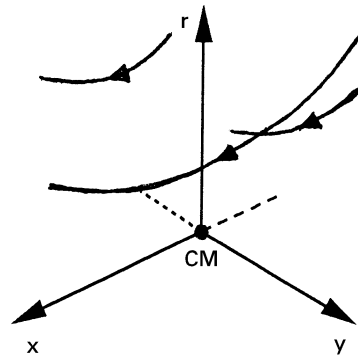

Fig. 10. The flow in the reduced phase space for $B=0$, $A<0$, and $h>0$.

5.3. The case $A<0$

This is the case of the repulsive inverse-square force (also known as the Coulomb force). If $h\leq 0$, relation (5.1) shows that every negative energy level in the reduced phase space is the collision-manifold point. Physically, the only solutions are those that rest at collision for all time. If $h>0$, every energy level in the reduced phase space is formed by a point (the collision-manifold point) and the upper sheet of a hyperboloid of two sheets (see Fig. 10). The integral $y=C$ foliates the surface in upper branches of hyperbola. There are no collision orbits except for those degenerate ones describing "motions" that start at collision, the particles sticking together for all time.

6. The flow for $B<0$

This is the case of a Manev-type force, in which collisions do not occur. The analysis depends on the sign of A.

6.1. The case $A>0$

In this case we distinguish three cases, depending on the sign of the energy constant h.

6.1.1. Negative energy

For $h<0$ we need to discuss three cases, depending on the sign of $h-A^2/(2B)$. If $h<A^2/(2B)$ the energy levels in the reduced phase space are imaginary ellipsoids, so real motion is impossible. If $h=A^2/(2B)$ the energy level in the reduced phase space is an equilibrium point E (see Fig. 11a), located at $r=-2B/A$, $x=y=0$. Physically, each equilibrium represents the body at rest at a distance $r=-2B/A$ from the center. If $h>A^2/(2B)$, every energy level in the reduced phase space is an ellipsoid (see Fig. 11b). The orbits are ellipses for $|y|<\sqrt{2B-A^2/h}$, which degenerate into the

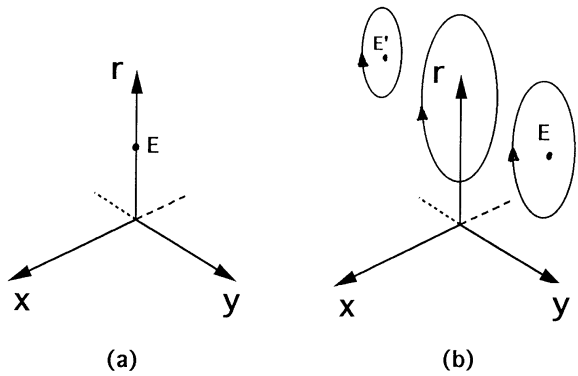

Fig. 11. The flow in the reduced phase space for $B<0$, $A>0$, and (a) $h=A^2/(2B)$ and (b) $A^2/(2B)<h<0$, respectively.

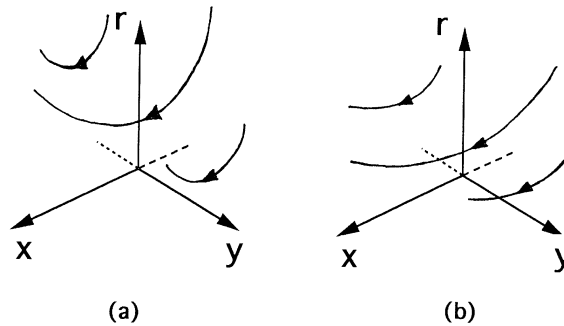

Fig. 12. The flow in the reduced phase space for $B<0$, $A>0$, and (a) $h=0$ and (b) $h>0$, respectively.

equilibria E and E', of coordinates $r=-A/h$, $x=0$, $y=\pm\sqrt{2B-A^2/h}$, if $|y|=\sqrt{2B-A^2/h}$. The equilibria correspond physically to stable orbits. The ellipses with $|y|>0$ correspond to the same periodic or quasiperiodic orbits on the torus as in Section 4.1.1, just that the precessional motion takes place in the opposite direction. The ellipse with $y=0$ corresponds physically to rectilinear periodic solutions: the body librates radially, i.e. moves back and forth along a line without escaping and without colliding with the center.

6.1.2. Zero energy

In this case the energy level in the reduced phase space is a paraboloid embedded in the half-space $r>0$ (see Fig. 12a). The orbits are parabolas. Physically, they represent precessional parabolas with zero asymptotic velocity at infinity. Note that the precessional motion has the opposite direction if compared to the one encountered in the case $B>0$, $A>0$, $h=0$. The parabola in the plane $y=0$ of the reduced phase space corresponds physically to rectilinear orbits; the body comes from infinity, stops at a

distance $r = -B/A$ from the center and then heads back to infinity with zero asymptotic velocity.

6.1.3. Positive energy

In this case every energy level in the reduced phase space is the upper sheet of a hyperboloid of two sheets (see Fig. 12b). The orbits are upper branches of hyperbola. Physically, the precessional orbits are hyperbolas and the asymptotic velocity at infinity is positive.

6.2. The case $A = 0$

This is the case of an inverse-cubic repulsive force. If $h \leq 0$, every energy level in the reduced phase space is either an imaginary ellipsoid or an imaginary cylinder, so no real motion is possible. If $h > 0$, every energy level in the reduced phase space has the similar physical interpretation as the orbits of the Section 6.1.3.

6.3. The case $A < 0$

This is a repulsive Manev force given by the sum of inverse-square and inverse-cubic forces. If $h \leq 0$, real motion is impossible. If $h > 0$, the situation is similar to the one of Section 6.2.3 above.

This completes the dynamical description of the generalized Manev problem in terms of the reduced phase space. However, the understanding of all dynamical aspects is far from over. Therefore, in the last section we will tackle the problem of block regularization, which will shed some light on the dynamics at and near collision.

7. Regularization of collisions

The notion of block-regularization was developed by Conley, Easton, and McGehee in the early 1970's [4, 12, 13, 22]. It occurred as a natural response to the old question about regularization of collision-solutions in the classical n-body problem, i.e. of the possible analytic continuation of the solution beyond the collision singularity (not to be mixed up with the regularization of the equations of motion, see [7]). Sundman [34] has shown first that this can be done for binary collisions; Siegel [32] has proved that, in general, triple collisions are not regularizable; and finally Saari [32] and Sperling [33] have shown that simultaneous binary collisions are regularizable. The idea of block-regularization occurred under the growing influence of the qualitative theory of dynamical systems in celestial mechanics. Its promoters asked whether the extension of the solution beyond collisions can be made with respect to nearby orbits in a meaningful way, i.e. if a natural property like continuity of solutions with respect to initial data is preserved after collision. This question is justified by physical applications, since we can never obtain 100%-accurate measurements: if continuity with respect to initial data is violated, physical measurements become meaningless. We will formally present the notion and then state and prove our results.

Let $\mathbf{M}$ be a smooth manifold, let $\mathbf{S}$ be a compact subset of $\mathbf{M}$, and let $\mathbf{F}$ be a vector field on $\mathbf{M}\backslash\mathbf{S}$. We call $\mathbf{S}$ the *singularity set* of the vector field $\mathbf{F}$. We denote by ϕ the *flow* of $\mathbf{F}$ on $\mathbf{M}\backslash\mathbf{S}$. The notion of *flow* is used loosely here since we do not require it to be defined for all values of the time variable t. Let $\mathbf{B}$ be a compact subset of $\mathbf{M}$ with nonempty interior and suppose that the boundary $\mathbf{b}$ of $\mathbf{B}$ is a smooth manifold such that $\mathbf{b}\cap\mathbf{S}=\emptyset$. Define the sets of *ingress*, *egress*, and *tangent* points with respect to the set $\mathbf{B}$:

$$\mathbf{b}^+=\{\mathbf{x}\in\mathbf{b}\mid\phi(\mathbf{x},(-\varepsilon,0))\cap\mathbf{B}=\emptyset \text{ for some } \varepsilon>0\},$$

$$\mathbf{b}^-=\{\mathbf{x}\in\mathbf{b}\mid\phi(\mathbf{x},(0,\varepsilon))\cap\mathbf{B}=\emptyset \text{ for some } \varepsilon>0\},$$

$$\mathbf{t}=\{\mathbf{x}\in\mathbf{b}\mid(\mathrm{d}/\mathrm{d}t)\phi(\mathbf{x},0) \text{ is tangent to } \mathbf{b}\}.$$

We call $\mathbf{B}$ an *isolating block* if $\mathbf{t}=\mathbf{b}^+\cap\mathbf{b}^-$. Denote by $\mathcal{O}(\mathbf{x})$ the orbits through $\mathbf{x}$:

$$\mathcal{O}(\mathbf{x})=\{\phi(\mathbf{x},t)\mid\phi(\mathbf{x},t) \text{ is defined}\}.$$

We say that an isolating block $\mathbf{B}$ isolates the singularity set $\mathbf{S}$ if $\mathbf{S}$ is contained in the interior of $\mathbf{B}$ and if $\mathcal{O}(\mathbf{x})$ is not fully contained in $\mathbf{B}$ for all $\mathbf{x}\in\mathbf{B}\backslash\mathbf{S}$. Let us further define the sets asymptotic to $\mathbf{B}$:

$$\mathbf{a}^+=\{\mathbf{x}\in\mathbf{b}^+\mid\phi(\mathbf{x},t)\in\mathbf{B} \text{ for all } t\geq 0 \text{ for which } \phi(\mathbf{x},t) \text{ is defined}\},$$

$$\mathbf{a}^-=\{\mathbf{x}\in\mathbf{b}^-\mid\phi(\mathbf{x},t)\in\mathbf{B} \text{ for all } t\leq 0 \text{ for which } \phi(\mathbf{x},t) \text{ is defined}\}.$$

By definition, if $\mathbf{x}\in\mathbf{b}^+\backslash\mathbf{a}^+$, then there exists a $t>0$ such that $\phi(\mathbf{x},t)$ does not belong to $\mathbf{B}$. Thus the time spent by the point $\mathbf{x}$ in the block can be defined by

$$T(\mathbf{x})=\inf_{t>0}\{\phi(\mathbf{x},t)\notin\mathbf{B}\}.$$

Let us remark that $\phi(\mathbf{x},[0,T(\mathbf{x})])\in\mathbf{B}$ and that $\phi(\mathbf{x},T(\mathbf{x}))\in\mathbf{b}^-$. We can now define the map across the block:

$$\Phi:\mathbf{b}^+\backslash\mathbf{a}^+\to\mathbf{b}^-\backslash\mathbf{a}^-,$$

$$\Phi(\mathbf{x})=\phi(\mathbf{x},T(\mathbf{x})).$$

Note that Φ is a diffeomorphism, as Conley and Easton [4] have proved.

Definition 7.1. We will say that the singularity set $\mathbf{S}$ is *block-regularizable* if there exists an isolating block $\mathbf{B}$ such that for the corresponding diffeomorphism $\Phi:\mathbf{b}^+\backslash\mathbf{a}^+\to\mathbf{b}^-\backslash\mathbf{a}^-$ there is a unique homeomorphism $\tilde{\Phi}:\mathbf{b}^+\to\mathbf{b}^-$, with $\tilde{\Phi}\equiv\Phi$ on $\mathbf{b}^+\backslash\mathbf{a}^+$.

It was McGehee in 1981 [23] who, while studying the two-body problem given by the inverse-α force law ($\alpha\geq 1$), recognized the importance of imposing the uniqueness condition on the extension function $\tilde{\Phi}$. This condition is indeed necessary since loss of uniqueness implies loss of continuity with respect to initial data.

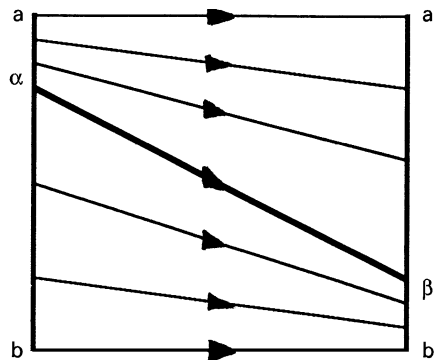

Fig. 13. The homeomorphism of $[a,b]$ into itself.

We can now prove the following general result:

Lemma 7.2. *Assume that for any isolating block* $\mathbf{B}$ *the corresponding diffeomorphism* $\Phi : \mathbf{b}^+\backslash\mathbf{a}^+ \to \mathbf{b}^-\backslash\mathbf{a}^-$ *is such that* $\mathbf{a}^+$ *and* $\mathbf{a}^-$ *contain a connected component of positive measure. Then the singularity* $\mathbf{S}$ *is not block-regularizable.*

Proof. Let $\mathbf{B}$ be an isolating block for which the corresponding diffeomorphism Φ can be extended to a homeomorphism $\tilde{\Phi}$ from $\mathbf{b}^+$ to $\mathbf{b}^-$, and let Ψ be the restriction of $\tilde{\Phi}$ to $\mathbf{a}^+$. It follows that Ψ is a homeomorphism from $\mathbf{a}^+$ to $\mathbf{a}^-$. Observe now that $\mathbf{a}^+$ and $\mathbf{a}^-$ are closed sets in the compact set $\mathbf{B}$, so they are themselves compact. We would like to show that since $\mathbf{a}^+$ and $\mathbf{a}^-$ contain a connected set of positive measure, there exist infinitely many homeomorphisms from $\mathbf{a}^+$ and $\mathbf{a}^-$ that are identical to Ψ if restricted (and corestricted) to the boundaries of $\mathbf{a}^+$ and $\mathbf{a}^-$. This will imply that there exist infinitely many extensions $\tilde{\Phi}$, so the collision-singularity set is not block-regularizable.

We first consider the case when $\mathbf{a}^+$ and $\mathbf{a}^-$ are one-dimensional. Since $\mathbf{a}^+$ and $\mathbf{a}^-$ have a connected component of positive measure, they are both homeomorphic to some interval $[a,b]$ and the boundaries of $\mathbf{a}^+$ and $\mathbf{a}^-$ correspond to a and b. So the problem of showing that there are infinitely many homeomorphisms from $\mathbf{a}^+$ to $\mathbf{a}^-$ that keep the boundaries of $\mathbf{a}^+$ and $\mathbf{a}^-$ fixed, reduces to showing that there are infinitely many homeomorphisms from $[a,b]$ to $[a,b]$ that send a to a and b to b. But this is obvious from Fig. 13, in which the correspondence is shown by arrows and each choice of the positions of α and β defines a different homeomorphism.

If $\mathbf{a}^+$ and $\mathbf{a}^-$ are two-dimensional, the problem reduces to squares instead of intervals, and the existence of infinitely many homeomorphisms is proved similarly. For n-dimensional sets $\mathbf{a}^+$ and $\mathbf{a}^-$, the problem reduces to n-dimensional hypercubes. This completes the proof.

Remark. *Things become more complicated in case the connectedness condition for* $\mathbf{a}^+$ *and* $\mathbf{a}^-$ *is removed, retaining only the positive-measure requirement. However, in the following application of Lemma* 7.2 *the connectedness condition will be fulfilled.*

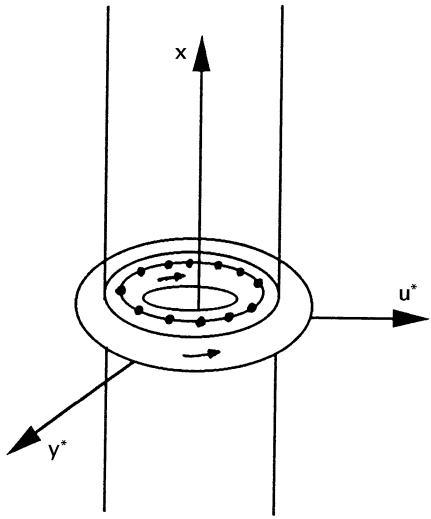

Fig. 14. The collision-manifold torus for $B>0$.

Theorem 7.3. *The singularity set of Manev-type problems given by potentials* $A/r + B/r^2$ *with* A, B *constants and* $B>0$, *is not block-regularizable.*

Proof. We will now represent the flow of system (3.2) in (x, y, u)-Coordinates. In Fig. 1a we saw that the collision manifold (for $r=0$) is a cylinder with the caps identified, i.e. a torus in some suitable (x, y^*, u^*)-coordinates (see Fig. 14). (By abuse, we will continue to work with (x, y, u)-coordinates, but imagine the torus representation.) Because of the integral (3.4), the solutions of system (3.2) (for $r \neq 0$) lie on cylinders, as Fig. 14 shows. The cylinders intersecting the torus contain only collision or ejection orbits, whereas the other cylinders contain only collisionless orbits.

The collision-manifold torus is in this case the singularity set, denoted by $\mathbf{S}$ at the beginning of this section. Any sphere around this torus is an isolating block $\mathbf{B}$, so isolating blocks do exist. But independently on its shape, an isolating block would be partitioned by $\mathbf{b}^+, \mathbf{b}^-$, and τ; moreover, the intersection between the set $\mathbf{B}$ and the cylinders that intersect the collision-manifold torus is homeomorphic to two annuli, one annulus for $\mathbf{a}^+$ and the other for $\mathbf{a}^-$. Consequently, $\mathbf{a}^+$ and $\mathbf{a}^-$ are connected and have positive measure. By Lemma 7.2, the singularity set is not block-regularizable. This completes the proof.

As it was shown by Easton [12], in the Newtonian case $A>0$, $B=0$ the singularity set, which has measure zero, is block-regularizable. However, this property gets lost in n-body problems ($n \geq 3$) for singularities involving a collision of at least three bodies.

As we have seen above, in the generic Manev-type case the singularity set is not block-regularizable even for binary collisions. This means that after an elastic bounce the future motion cannot be predicted, which is in fact the case in the astronomical reality (even if it mainly happens for other reasons: the bodies are not point-masses, collisions are not purely elastic, energy is not preserved after collision, etc.). So, beyond

the argument given in Section 1, this seems to be another point favoring a better suitability of the original Manev model to the realities of the solar system, if compared to what the classical Newtonian model offers.

References

[1] R. Adler, B. Bazin, M. Schiffer, Introduction to General Relativity, McGraw-Hill, New York, 1975.
[2] V.A. Brumberg, Present problems in relativistic celestial mechanics, in: J. Kovalevski, V.A. Brumberg (Eds.), Relativity in Celestial Mechanics and Astrometry, Proc. 114th Symp. of the IAU, Leningrad, 1985, Dordrecht, Boston, 1986, pp. 5–17.
[3] J. Casasayas, E. Fontich, A. Nunes, Transversal homoclinic orbits for a class of Hamiltonian systems, in: Hamiltonian Systems and Celestial Mechanics, Advanced Series in Nonlinear Dynamics, vol. 4, World Scientific, Singapore, 1993, pp. 35–44.
[4] C. Conley, R. Easton, Isolated invariant sets and isolating blocks, Trans. Amer. Math. Soc. 158 (1) (1971) 35–61.
[5] S. Craig, F.N. Diacu, E. Lacomba, E. Perez, The anisotropic Manev problem, submitted.
[6] J. Delgado, F.N. Diacu, E.A. Lacomba, A. Mingarelli, V. Mioc, E. Perez, C. Stoica, The global flow of the Manev problem, J. Math. Phys. 37 (6) (1996) 2748–2761.
[7] F.N. Diacu, Regularization of partial collisions in the *n*-body problem, Differential Integral Equations 5 (1) (1992) 103–136.
[8] F.N. Diacu, The planar isosceles problem for Maneff's gravitational law, J. Math. Phys. 34 (12) (1993) 5671–5690.
[9] F.N. Diacu, Near-collision dynamics for particle systems with quasihomogeneous potentials, J. Differential Equations 128 (1996) 58–77.
[10] F.N. Diacu, P. Holmes, Celestial Encounters – The Origins of Chaos and Stability, Princeton Univ. Press, Princeton, NJ, 1996.
[11] F.N. Diacu, A. Mingarelli, V. Mioc, C. Stoica, The Manev two-body problem: quantitative and qualitative theory, in: Dynamical Systems and Applications, World Scientific Series in Applicable Analysis, vol. 4, World Scientific, Singapore, 1995, pp. 213–227.
[12] R. Easton, Regularization of vector fields by surgery, J. Differential Equations 10 (1971) 92–99.
[13] R. Easton, Isolating blocks and symbolic dynamics, J. Differential Equations 17 (1975) 96–118.
[14] A. Einstein, L. Infeld, B. Hoffmann, The gravitational equations and the problem of motion, Ann. Math. 39 (1) (1938) 65–100.
[15] H. Goldstein, Classical Mechanics, Addison-Wesley, Reading, MA, 1980.
[16] E.A. Lacomba, J. Llibre, A. Nunes, Invariant tori and cylinders for a class of perturbed Hamiltonian systems, in: T. Ratiu (Ed.), The Geometry of Hamiltonian Systems, Proc. Workshop 5–16, June 1989, Springer Verlag, New York, 1991.
[17] T. Levi-Civita, Le Problème des *n* corps en relativité générale, Mémorial des Sciences Mathématiques, Fascicule CXVI, Gauthiers-Villars, Paris, 1950.
[18] G. Maneff, La gravitation et le principe de l'égalité de l'action et de la réaction, C. R. Acad. Sci. Paris 178 (1924) 2159–2161.
[19] G. Maneff, Die Gravitation und das Prinzip von Wirkung und Gegenwirkung, Z. Phys. 31 (1925) 786–802.
[20] G. Maneff, Le principe de la moindre action et la gravitation, C. R. Acad. Sci. Paris 190 (1930) 963–965.
[21] G. Maneff, La gravitation et l'énergie au zéro, C. R. Acad. Sci. Paris 190 (1930) 1374–1377.
[22] R. McGehee, Triple collision in the collinear three-body problem, Invent. Math. 27 (1974) 191–227.
[23] R. McGehee, Double collisions for a classical particle system with nongravitational interactions, Comment. Math. Helvetici 56 (1981) 524–557.
[24] V. Mioc, C. Stoica, Discussion et résolution complète du problème des deux corps dans le champ gravitationnel de Maneff, C. R. Acad. Sci. Paris sér.I, 320 (1995) 645–648.
[25] V. Mioc, C. Stoica, Discussion et résolution complète du problème des deux corps dans le champ gravitationnel de Maneff (II), C. R. Acad. Sci. Paris sér.I 321 (1995) 961–964.

[26] R. Moeckel, A nonintegrable model in general relativity, Commun. Math. Phys. 150 (1992) 415–430.
[27] F.R. Moulton, An Introduction to Celestial Mechanics (2nd revised Ed.), Dover, New York, 1970.
[28] C. Robinson, Dynamical Systems: Stability, Dynamical Systems, and Chaos, CRC Press, Boca Raton, FL, 1995.
[29] D.G. Saari, Regularization and the artificial earth satellite problem, Celest. Mech. 9 (1974) 55–72.
[30] D.G. Saari, The manifold structure for collision and for hyperbolic-parabolic orbits in the *n*-body problem, J. Differntial Equations 55 (1984) 300–329.
[31] K. Schwarzschild, Über das Gravitationsfeld eines Massenpunktes nach der Einsteinschen Theorie, Sitzber. Preuss. Akad. Wiss., Berlin, 1916, pp. 189–196.
[32] C.L. Siegel, Der Dreierstoss, Ann. Math. 36 (1912) 105–179.
[33] H.J. Sperling, On the real singularities of the *n*-body problem, J. Reine Angew. Math. 245 (1970) 15–40.
[34] K. Sundman, Mémoire sur le problème des trois corps, Acta Math. 36 (1912) 105–179.
[35] E.T. Whittaker, A Treatise on the Analytical Dynamics of Particles and Rigid Bodies, 4th ed., Cambridge Univ. Press, 1937.
[36] A. Wintner, The Analytical Foundations of Celestial Mechanics, Princeton Univ. Press, Princeton, NJ, 1941.